Carbohydrate Polymers 86 (2011) 1468–1475

Contents lists available at ScienceDirect

Carbohydrate Polymers

journal homepage: www.elsevier.com/locate/carbpol

Extraction of nanocellulose fibrils from lignocellulosic fibres: A novel approach

E. Abraham[a], B. Deepa[a], L.A. Pothan[a,*], M. Jacob[c], S. Thomas[b], U. Cvelbar[d], R. Anandjiwala[c]

[a] Department of Chemistry, Bishop Moore College, Mavelikkara 690 101, Kerala, India
[b] School of Chemical Sciences, Mahatma Gandhi university, Kottayam 686 560, Kerala, India
[c] Fibres and Textiles Competence Area, CSIR, Materials Science and Manufacturing, PE, South Africa
[d] Jozef Stefan Institute, Jamova cesta 39, SI-1000 Ljubljana, Slovenia

ARTICLE INFO

Article history:
Received 12 May 2011
Accepted 14 June 2011
Available online 21 June 2011

Keywords:
Natural fibres
Steam explosion
Extraction
Nanocellulose

ABSTRACT

The objective of this work was to develop a simple process to obtain an aqueous stable colloid suspension of cellulose nano fibrils from various lignocellulosic fibres. For the preliminary analysis we have studied three different fibres: banana (pseudo stem), jute (stem) and pineapple leaf fibre (PALF). To study the feasibility of extracting cellulose from these raw fibres we have adopted steam explosion technique along with mild chemical treatment. These processes included usual chemical procedures such as alkaline extraction, bleaching, and acid hydrolysis but with a very mild concentration of the chemicals. The chemical constituents of the fibre in each processing step were determined by ASTM standard procedures. Morphological, spectroscopic and thermal analyses of the fibres were carried out and found that the isolation of cellulose nanofibres occurs in the final step of the processing stage and they possess improved thermal stability for various advanced nanotechnological applications.

1. Introduction

In nature, a large number of plants and animals synthesize extra-cellular high-performance skeletal biocomposites consisting of a matrix reinforced by fibrous biopolymers (Mohanty, Misra, & Hinrichsen, 2000). Cellulose is a classical example where the reinforcing elements exist as whisker-like microfibrils that are biosynthesized and deposited in a continuous manner (Itoh & Brown, 1984). It is the world's most abundant natural renewable biodegradable polymer and has been estimated that globally around 10^{12} tonnes are synthesized and also destroyed each year (Hon, 1994). The development of low-cost, sustainable, and renewable resources is critical to meet the growing environmental concerns and energy demands. Most lignocellulosic biomass comprises mainly cellulose, hemicellulose, and lignin. Due to its heterogeneity and crystallinity, however, direct utilization of biomass by microbes is extremely slow. Efficient separation of constitutive biomass components constitutes one of the major obstacles to the efficient utilization of renewable resources. However, such separation is mandatory for its effective utilization in the current nanotechnological field and of the various pre-treatment technologies for the isolation of nanocellulose fibres, steam explosion is an attractive choice.

As described in some comprehensive reviews, the fabrication of nanofibres, generally defined as fibres with a diameter below 100 nm (Xia et al., 2003) is presently the subject of much attention because of their unique characteristics such as a very large surface-to-volume ratio (Huang, Zhang, Kotaki, & Ramakrishna, 2003) and the formation of a highly porous mesh as compared with other commercial fibres. A large number of synthesis and fabrication methods for producing these nanofibres have already been reported. It is well-known that nanofibres are produced in nature, for example, collagen fibrils in tendons and ligaments and silk fibroin. Among the variety of natural nanofibres, cellulose microfibrils, which are the major constituent of plant cell walls and are also produced by some bacteria, are the most abundant natural nanofibre on earth. Cellulose is a polydispersed linear polymer of β-(1,4)-D-glucose units with a syndiotactic configuration. Cellulose chains aggregate to form microfibrils, long thread like bundles of molecules stabilized laterally by hydrogen bonds between hydroxyl groups and oxygen's of adjacent molecules (Nishiyama, Sugiyama, Chanzy, & Langan, 2003; Subramanian, Kononov, Kang, Paltakari, & Paulapuro, 2008). In the structure of a natural fibre, the molecular arrangement of these microfibrillar bundles is sufficiently regular that cellulose exhibits a crystalline X-ray diffraction pattern. The resultant stable structure has outstanding mechanical properties, including a high Young's modulus (138 GPa in the crystal region along the longitudinal direction) and a very low coefficient of ther-

* Corresponding author. Tel.: +91 479 2301730.
E-mail address: lapothan@gmail.com (L.A. Pothan).

0144-8617/$ – see front matter © 2011 Elsevier Ltd. All rights reserved.
doi:10.1016/j.carbpol.2011.06.034

mal expansion (10^{-7} K^{-1} along the longitudinal direction) (Nishino, Matsuda, & Hirao, 2004). Therefore, cellulose whiskers and fibrils have great potential for use as reinforcement in nanocomposites and have attracted a great deal of interest recently. In addition to their exceptional mechanical properties, cellulose nanofibres have been shown to be an ideal reinforcement of transparent resins since they are free from light scattering due to their diameters being less than one-tenth of the visible light wavelength (Novak, 2005).

Since plant-based cellulose nanofibres have the potential to be extracted into fibres thinner than bacterial cellulose, many researchers have been extensively studying the extraction of nanofibres from wood and other plant fibres. In cell walls, cellulose nanofibres are embedded in matrix substances such as hemicellulose and lignin, and, up unto this time, the removal of the matrix substances has been performed before the fibrillation process. Bleached pulps are often used in order to skip the matrix removal process (Turbak, Synder, & Sandberg, 1983). The fibrillation of plant fibres was achieved by mechanical treatments using high-pressure homogenizer, a grinder (Chakraborty, Sain, & Kortschot, 2005), cryocrushing (Taniguchi & Okamura, 1998), etc. Recently some researchers adopted ultrasonic (Zhao, Feng, & Gao, 2007) and enzymatic pre-treatment methods (Paakko et al., 2007) for the preparation of nanofibres. However, because of the complicated multilayered structure of plant fibres and the interfibrillar hydrogen bonds, the fibrils obtained by these methods are aggregated nanofibres with a wide distribution in width. Studies were done to prepare cellulose microfibrils from sugar beet, tunicin, etc. But cellulose microfibrils obtained from these sources had some disadvantages. Bacterial cellulose microfibrils are very expensive and can cause a contamination problem in alimentary applications (Bhatnagar & Sain, 2005). It is reported that TEMPO-mediated oxidation on the surface of the microfibrils assisted the homogenizing mechanical treatment and enabled them to obtain nanofibres with a uniform width of 3–5 nm (Saito, Nishiyama, Putaux, Vignon, & Isogai, 2006). They used strong acids with high concentration of 70–80% for the preparation of nanofibres from natural fibres. They tend to be toxic and the degradation of cellulose was found in them. We used mild acids with low concentration (5% oxalic acid) which overcome toxicity, with no degradation of cellulose. Here we report on an efficient extraction of cellulose nanofibres from natural fibres like banana, jute and pineapple leaf fibre as they exist in the cell wall, by a mild chemical treatment followed by very simple mechanical treatment.

2. Experimental

2.1. Materials

Raw banana, jute and pineapple leaf fibres were obtained from YMCA Marthandom, Tamil Nadu, India. The various chemicals used for extraction of fibre and the preparation of nanocellulose are ethanol, diethyl ether, sulphuric acid, $KMnO_4$, NaOCl, NaOH, acetic acid, oxalic acid, etc. and all are from Nice Chemicals, Cochin, India. All reagents used were of analytical grade.

2.2. Methods for the isolation of nanocellulose from raw fibres

2.2.1. Step 1. Alkali treatment of the fibre

The optimum alkali treatment is both a very effective surface modification and a low cost surface treatment of natural fibres. Banana, pineapple leaf fibre (PALF) and jute fibres were soaked with 2% caustic soda and placed for 6 h at a temperature of 30 °C.

2.2.2. Step 2. Steam explosion of the mercerized fibre

Steam explosion technique was applied on the mercerized fibre at a pressure of 137 Pa (20 lbs) for 1 h. Steam pre-treatment is performed by loading the lignocellulosic material directly into the steam gun and treating it with high pressure steam at temperatures within 200–250 °C. Substrates are then recovered by water washing where a typical flow-sheet for pre-treating and fractionating lignocellulosic residues is presented. The paper refers 'steam exploded fibre' which means the alkali treatment followed by steam exploded fibre.

Steam explosion apparatus: We have used a laboratory autoclave which can work with 137 Pa (20 lbs) pressure for the steam explosion process.

2.2.3. Step 3. Bleaching of the steam exploded fibre

Mercerized, steam exploded sample is then subjected to bleaching. After the successive chemical treatments, the bleaching treatment with a chlorine dioxide ($NaClO_2$) solution (pH 2.3) for 1 h at 50 °C was performed to remove the remained lignin. In the bleaching step, the absence of elemental chlorine is accomplished by using $NaClO_2$.

2.2.4. Step 4. Acid treatment followed by steam explosion

The bleached sample is then subjected to mild acid treatment. 5% oxalic acid was used for the acid hydrolysis and followed by second step of steam explosion for 1 h. 137 Pa (20 lbs) pressure was used followed by sudden release of pressure. The fibres were then washed thoroughly by water and then subjected to mechanical stirring followed by sonication.

2.3. Chemical analysis

Chemical constituent of fibres was determined according to ASTM standards. α-Cellulose (ASTM D 1103-55T), hemicellulose (ASTM D 1104-56), lignin (ASTM D 1106-56), moisture content (ASTM D 4442-92). The cellulose, hemicellulose, lignin and moisture contents of the fibre in the untreated raw, steam exploded and acid hydrolysed stages were determined.

2.4. Fourier transfer-infra red (FTIR) spectroscopy

Fourier transfer-infra red spectroscopy (FTIR) spectra of the fibres were recorded by a Shimadzu IR-470 IR spectrophotometer. About 2 mg of fibre was crushed into small particles in liquid nitrogen. The fibre particles were then mixed with KBr and pressed into a small disc about 1 mm thick.

2.5. X-ray diffraction (XRD) technique

X-ray equatorial diffraction profiles of the fibres were collected by a JEOL diffractometer, Model JDX 8P, using CuKα radiation at the operating voltage and current of 30 kV and 20 mA, respectively. The diffraction intensities were recorded between 2 and 80° (2θ angle range).

2.6. Scanning electron microscopy (SEM)

Morphological analysis of untreated and steam exploded fibres was done by scanning electron microscopy. SEM micrographs of fibre surface were taken using a scanning electron microscope model JEOL JSM-35C and Cambridge 250 MK_3 stereo scan operated at 20 kV. Prior to SEM evaluation, the samples were coated with platinum by means of a plasma sputtering apparatus.

2.7. Scanning probe microscopy (SPM)

The morphological study of the final nanocellulose fibrils was done by scanning probe microscopy. The scanning probe microscopy images of the nanofibres were made with a Multimode SPM (Veeco Inc., Santa Barbara, USA) with a Nanoscope IV controller in tapping mode.

2.8. Thermo gravimetric analysis (TGA)

TGA analyses were carried out using a Mettler TG 50 module attached to a Mettler TC 11 4000 thermal analyzer (Switzerland). The thermal analyses were done in a nitrogen atmosphere under a flow rate of 100 mL/min using an alumina crucible with a pinhole. A constant heating rate of 5 °C/min was maintained.

3. Results and discussion

The alkali treatment removes a certain amount of lignin, hemicellulose, wax and oils covering the external surface of the fibre cell wall, depolymerises the native cellulose structure, defibrillates the external cellulose microfibrils and exposes short length crystallites. The mercerized fibre is then subjected to steam explosion treatment. The steam-treated material is then obtained by rapid depressurization of the vessel causing the material to expand (explode) into a stainless steel cyclone. Hence, this sudden pressure drop (explosion) can disrupt or defibrillate the pre-treated material whose structure has been softened through mercerization followed by high pressure steaming.

Bleaching of the steam exploded fibre was done for complete elimination of the remaining cementing materials from the fibre. Hemicellulose is a water soluble polysaccharide. Lignin is a complex organic compound with alkali soluble character. Hence the percentage of lignin decreases from raw fibre to bleached fibre.

After cellulose was prepared, acid hydrolysis was carried out in order to produce cellulose nano fibrils. Oxalic acid will react with sodium derivative of the fibre to form the pure cellulose. The samples were further broken down into leaner fragments by the sonicator. The slurry obtained after the sonication exhibited a remarkably high viscosity. It suggested that the synthesis of homogeneous dispersion of hydrophilic cellulose nano fibrils in water from natural fibres has been accomplished. The process provided high turbulence and shear that created the efficient mechanism of reduction in size nanocellulose level.

Table 1 describes the chemical composition of the three studied fibres at different processing stages. The percentage of crystalline cellulose increases when treated with NaOH followed by steam explosion process. The fine structure of cellulose materials is composed of crystalline and amorphous regions. The amorphous regions easily absorb chemicals such as dyes and resins, whereas the compactness of the crystalline regions makes it difficult for chemical penetration (Klemm, Philipp, Heinze, Heinze, & Wagenknecht, 2004). The modification of plant fibres may involve the removal of the surface impurities, the swelling of the crystalline region, and removal of the hydrophilic hydroxyl groups. The common trend from the observation is the gradual decrease of amorphous components like lignin and hemicellulose from raw fibre to bleached fire. The lignin will react with $NaClO_2$ and dissolve out as lignin chloride. The percentage increase of the pure cellulose component with each processing step is another main observation.

Moisture content shows a gradual increase from raw to bleached fibre. This is due to the increase in percentage of cellulose content during the process. Since in pure cellulose, each unit has three free –OH groups, the moisture absorption rate increases with cellulose content. Also during alkali treatment, the swelling of the fibre takes place, which also promotes the absorption of moisture by capillary action. The mercerization (alkali treatment) of the fibre will lead to the swelling which facilitates the breakdown during acid hydrolysis. Acid hydrolysis of cellulose leads to hydrolytic cleavage of glycosidic bond between two anhydroglucose units. Thus the amorphous portion gets dissolved by acid hydrolysis, leaving behind the crystalline regions. Acid hydrolysis followed by mechanical treatment (sonication) results in disintegration of the cellulose structure into micro and nanocrystalline forms (Klemm et al., 2004).

3.1. FTIR analysis

The infrared spectra of cellulose, hemicellulose and lignin (Erdtman, 2003) were studied in the literature. The three materials are mainly composed of alkanes, esters, aromatics, ketones and alcohols, with different oxygen-containing functional groups. Infrared transmittance spectra with main observed peaks of the three studied fibres in different stages are shown in Table 2. All samples presented two main transmittance regions. Lignin presented characteristic peaks in the range 1200–1300 cm^{-1} corresponding to the aromatic skeletal vibration. In addition, due to the presence of functional groups such as methoxyl-O-CH_3, C–O–C and aromatic C=C, peaks in the region between 1830 cm^{-1} and 1730 cm^{-1} were observed (Reddy & Yang, 2005). The –OH bending (Lojewska, Miskowiec, Lojewski, & Pronienwicz, 2005) of adsorbed water at 1640 cm^{-1} is reported. All the FTIR spectra were developed after the same carefully drying process, however the water adsorbed in the cellulose molecules is very difficult to extract due to the cellulose–water interaction. The peak present at 1730–1740 cm^{-1} in the spectrum corresponding to the raw fibres could be due to the presence of C=O linkage, which is a characteristic group of lignin and hemicellulose, at 1765–1715 cm^{-1}. Another possibility is that carboxyl or aldehyde absorption could be arising from the opened terminal glycopyranose rings or oxidation of the C–OH groups. Alkali treatment reduces hydrogen bonding due to removal of the hydroxyl groups by reacting with sodium hydroxide. This results in the increase of the –OH concentration, evident from the increased intensity of the peak between 3300 and 3500 cm^{-1} bands compared to the untreated fibre (Lojewska et al., 2005; Mwaikambo & Ansell, 1999).

It is reported that in most lignified plant cells lignin and hemicellulose are deposited between the microfibrils to give an interrupted lamellar structure and without the removal of these noncellulosic components, the cellulose I to cellulose II transformation will be restricted. With the treatment of NaOH and bleaching agents, the lignin is removed and in this case also the degree of crystallinity goes on increasing. This may be due to the removal of lignin which acts as a cementing material and on delignification, an ordered arrangement of the crystalline cellulose in the structure takes place.

From the FTIR analysis it has been concluded that there is a reduction in the quantum of binding components present in the fibres due to the process of steam and chemical treatment. The raw fibres have a characteristic peak in between 1730–1740 cm^{-1} and 1200–1300 cm^{-1}. These peaks are chiefly responsible for the hemicellulose and lignin components. These characteristic peaks are completely absent in the final bleached cellulose fibre.

3.2. X-ray diffraction analysis

Fig. 1(a) and (b) shows the X-ray diffraction analysis of the banana and PALF, respectively. On removing the noncellulosic constituents of the fibres by chemical treatment, the degree of crystallinity and crystallinity index will change. The fibre constitutes crystalline and amorphous regions. The degree of crystallinity, i.e., the amount of crystalline cellulose present in a cellulosic fibre cannot be exactly defined, as neither the crystalline portions are

Table 1
Constituents of the fibres in different stages.

	Cellulose (%)	Hemicellulose (%)	Lignin (%)	Moisture content (%)
Raw banana fibre	69.9	19.6	5.7	9.8
Raw PALF	75.3	13.3	9.8	9.0
Raw jute fibre	68.3	15.4	10.7	10.1
Steam exploded banana fibre	88.3	6.9	2.9	10.1
Steam exploded PALF	89.8	4.9	2.5	9.3
Steam exploded jute fibre	86.7	4.3	3.5	10.4
Bleached banana fibre	96.8	0.2	0.2	9.3
Bleached PALF	97.3	0.2	–	8.9
Bleached jute fibre	97.3	–	–	9.6

Table 2
Infrared transmittance peaks (cm^{-1}) of the fibres in different stages.

	FTIR (cm^{-1}) spectra (%T)						
	–OH stretching	C–H vibration	C=O stretching	Absorbed water	C–H stretching	Aromatic ring vibration of lignin	C–C stretching
Raw banana	3400	2923	1736	1638	1369	1247	1029
Raw PALF	3432	2922	1738	1617	1372	1238	1020
Raw jute	3381	2919	1736	1633	1376	1245	1019
Steam exploded banana fibre	3397	2924	1735	1625	1369	–	1020
Steam exploded PALF	3424	2922	1738	1617	1372	–	1022
Steam exploded Jute	3346	2919	1736	1633	1376	–	1019
Bleached banana fibre	3390	2922	–	1607	1370	–	1019
Bleached PALF	3412	2920	–	1655	1353	–	1022
Bleached jute	3316	2924	–	1607	–	–	1019

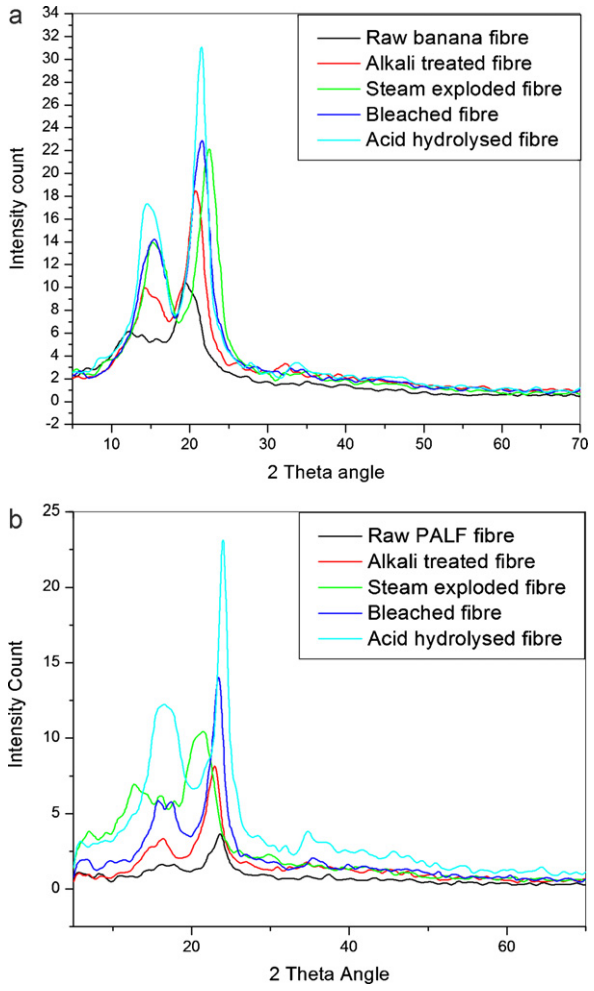

Fig. 1. XRD analysis of (a) banana fibre and (b) PALF fibre.

perfect crystals nor the noncrystalline portion completely disordered. Alkalization of plant fibres changes the surface topography of the fibres and their crystallographic structure. The removal of surface impurities on plant fibres is advantageous in fibre–matrix adhesion, as it facilitates both mechanical interlocking and the bonding reaction due to the exposure of the hydroxyl groups to chemicals such as resins and dyes. Apart from truly crystalline and truly amorphous, there are some regions of intermediate order where the molecular configuration is liable to change by the chemical treatment. The effect of alkali and acid treatment of the fibre surface was studied by XRD. XRD analysis of the alkali treated fibres also revealed an increase in the crystallinity index of the banana, PALF and jute. Other researchers have noted an improvement in the order of the crystallites as the cell wall thickens upon alkali treatment (Mwaikambo & Ansell, 1999). The crystallinity index initially increases but then declines at high alkali concentrations when damage to the cell wall occurs.

Alkali treatment of the natural fibre will lead to the swelling of the fibre and subsequent increase in the absorption of moisture. Treatment with alkali leads to the removal of cementing materials like lignin, hemicellulose and pectin which will result in the increase of percentage crystallinity of the fibre. With an increase in acid concentration up to 10% an increase in crystallinity was observed. However when the acid concentration was increased to 50% a decrease in the concentration of the pure cellulose was found showing that at high concentration the pure cellulose will degrade. The trend is same in all fibres which we studied (banana, pineapple leaf fibre and jute). We can also see that the percentage crystallinity is of the order PALF > banana > jute. This order agrees with the values of cellulose content determined in these samples.

The XRD graphs of studied fibres show that they are in a crystalline nature. In raw fibre, crystalline cellulose components are oriented in the matrix of lignin, hemicellulose, pectin, etc. During chemical treatment the cementing materials (matrix) will be dissolved, and the remaining pure crystalline particles isolated. These particles show increasing orientation along a particular axis, due to their similarity in shape. These pure crystalline particles show increasing orientation along a particular axis as the fibres

Table 3
The crystallinity index of the fibres.

Material	Crystallinity index (I_c)
Raw banana fibre	10.5
Raw PALF	11.3
Raw jute fibre	9.1
Steam exploded banana fibre	54.1
Steam exploded PALF	63.7
Steam exploded jute fibre	52.9
Bleached banana fibre	83.8
Bleached PALF	89.3
Bleached jute fibre	88.6

are treated under different processing conditions. The effect of various treatments on the crystallinity of the fibres was also calculated. Table 3 shows the values of the crystallinity index obtained in the case of variously treated fibres.

The crystallinity index of the fibre can be calculated using the formula$$\text{Crystallinity index} = \left\{ \frac{I_{\text{crystalline}} - I_{\text{amorphous}}}{I_{\text{crystalline}}} \right\} \times 100$$

The crystallinity was found to vary depending on the conditions applied. The maximum crystallinity was obtained when acid hydrolysis was carried out to the bleached fibre. In natural cellulose fibres, the regions of intermediate order in the structure play an important role in the determination of the degree of crystallinity.

From the peak intensity of the variously treated fibres that were observed, it has been found that acid hydrolysis changes the fibre diameter as well as the crystallinity. It could be noticed that cellulose was present in the form of cellulose I, and not cellulose II, which arises from the fact that there is no shift of the main peak upon mercerization (Bhatnagar & Sain, 2005). In case of jute fibre during acid treatment, the pure cellulose is isolated more when the concentration of the oxalic acid increases up to 20%. Moreover, in the process of hydrolysis, the hydronium ions could penetrate into the amorphous regions of cellulose promoting the hydrolytic cleavage of glycosidic bonds and finally releasing the individual crystallites (Nishiyama, Langan, & Chanzy, 2002).

It is reported that in most lignified plant cells lignin and hemicellulose are deposited between the microfibrils to give an interrupted lamellar structure and without the removal of these noncellulosic components, the cellulose I to cellulose II transformation will be restricted. It is well-known that cellulose has four polymorphs, cellulose I, II, III, and IV, which are distinguishable by X-ray diffraction (Isogai, Usuda, Kato, Uryu, & Atalla, 1989). Cellulose I is the crystal form of native cellulose. Cellulose II is generally formed in regenerated cellulose or mercerized cellulose. The cellulose present in the raw fibres is in cellulose I form and upon alkali treatment, we are expecting a polymorphic modification of the crystalline state of the samples from cellulose I to cellulose II (Kim, Imai, Wada, & Sugiyama, 2006). It is reported that the crystalline transformation in natural fibres happens with an alkali concentration of up to 32% (8 N) and we are using only 2% of NaOH. Further the mercerization step is one of the first stages of the extraction process which permits the accessibility of mercerization to the peripheral part of the fibres and the cementing materials in the raw fibres. The lower concentration of alkali and the limited accessibility to the cellulose molecules reduce the crystalline transformation of cellulose polymorphs. Even though some transformation has happened in the PALF which has highest cellulose content and this polymorphic change is visible from the shift in the main peak of the XRD of steam exploded PALF to left from the raw fibre diffractogram. But this transformation is not retained up to the final stage of the extraction process since upon oxalic acid treatment the cellulose II is again back to cellulose I which is evident from the nanocellulose XRD.

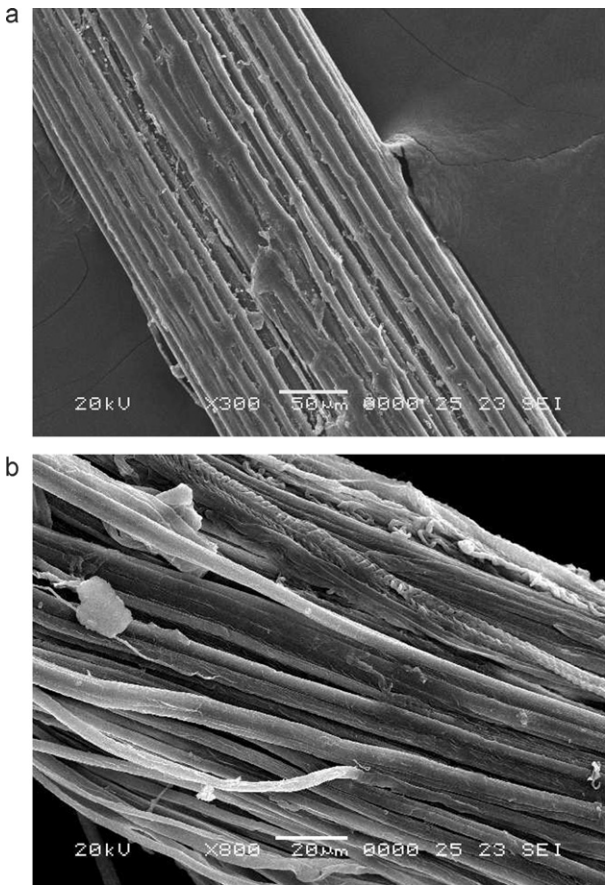

Fig. 2. SEM of (a) raw PALF and (b) steam exploded PALF.

A detailed polymorphic transformation upon the mercerization of these fibres will be discussed in another paper.

It has been concluded from the X-ray diffractograms that as banana, PALF and jute fibres undergo steam explosion, bleaching and further acid hydrolysis there is a decrease in the fibre diameter. As the acid concentration is increased there is decrease in the fibre size.

3.3. Morphological analysis by SEM and SPM

Fig. 2(a) and (b) shows the SEM micrographs of the untreated raw PALF. Fig. 2(b) shows the SEM micrographs of the steam exploded PALF. The clear demonstration of the defibrillation and depolymerisation by steam explosion is seen in this figure. The removal of the surface impurities along with defibrillation is shown from the figure. Fig. 3(a) shows the SPM micrographs of the untreated raw banana fibre. Each fibre is composed by several microfibrils with diameters in the range of 3–12 μm. Each elementary fibre shows a compact structure; exhibiting an alignment in the fibre axis direction with some non-fibrous components in the fibre surface (Garcıa, Jaldon, Dupeyre, & Vignon, 1998). It was previously shown that during the chemical treatment (alkalization) most of the lignin and hemicellulose were removed. Mechanical treatment (steam explosion) further removed the amorphous materials (lignin, hemicellulose, etc.) from the inner part of the fibre via depolymerisation and defibrillation. Fibre diameter was again reduced in the acid hydrolysis followed by steam explosion and pure cellulose fibre with a diameter of less than 100 nm was obtained. Thus cellulose microfibrils of the original fibres were separated from each other to produce fibrils with diameters around 5–50 nm. The scanning probe microscopy (SPM) pictures show the

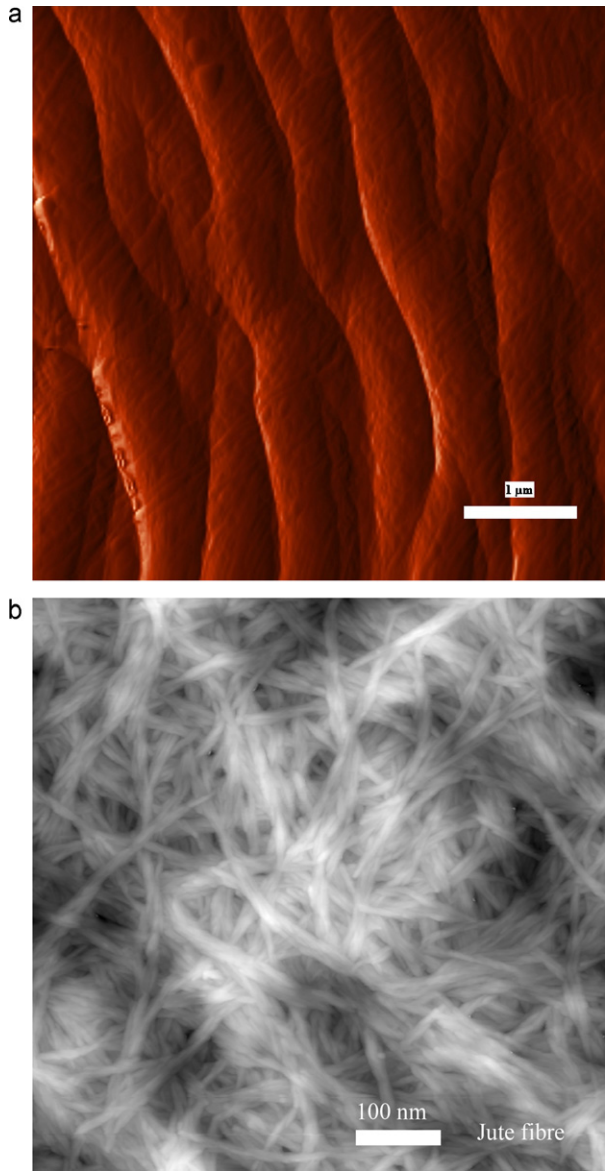

Fig. 3. SPM of (a) raw banana fibre and (b) jute nano dispersion.

final cellulose nano fibrils with diameters of 5–50 nm. Fig. 3(b) shows the SPM image of the cellulose nano dispersions of jute fibre. The birefringence study is also conducted by using *polarographic* method and the result shows a clear birefringence for all the three dispersions at dilute concentrations. The size distribution of the nanocellulose fibres in the dispersion of jute fibre is calculated and found that majority of the nanocellulose fibres present in the dispersion are in the range of 15–25 nm in diameter irrespective of the type of the fibres.

3.4. The element detection analysis

Element detection analysis was carried out by EDS technique of the scanning electron microscopic instrument in liquid nitrogen atmosphere. This analysis reveals the presence of various elements present in the focussed area of the fibre. A characteristic observation of the result is the weight percentage of the carbon and oxygen in the raw fibres. Pure cellulose has a higher weight percentage for oxygen than carbon. But in untreated raw jute and PALF, there is a higher weight percentage for carbon than oxygen. The high percentage of the lignin content is responsible for the result. Lignin has

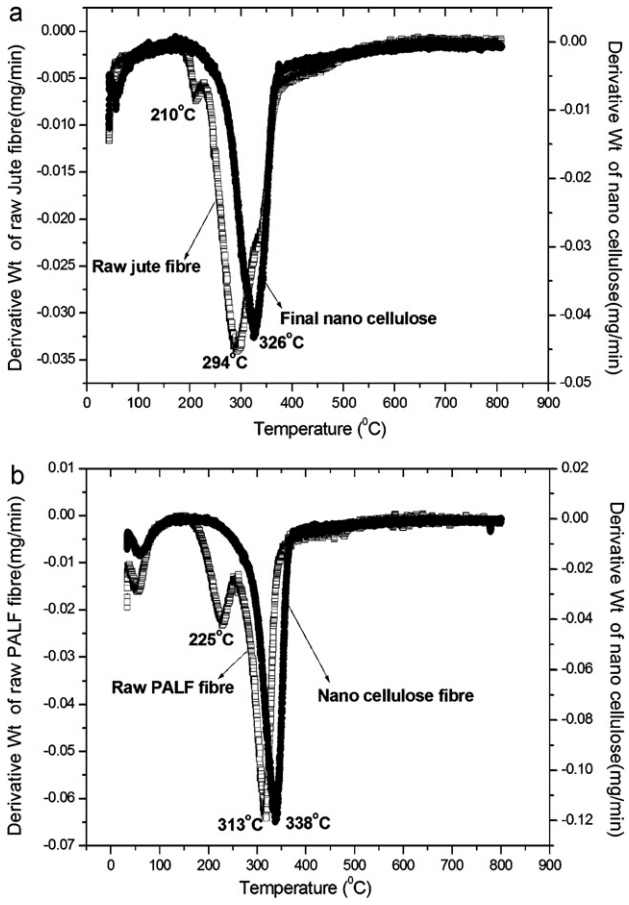

Fig. 4. DTG of (a) jute fibre and (b) PALF.

an aromatic structure with very high carbon content than cellulose and hemicellulose. The lignin decomposition and elimination are clearly demonstrated from the result obtained in the weight percentage of carbon and oxygen of the bleached fibre. All bleached fibres show a higher oxygen weight percentage than carbon.

3.5. Thermal studies of the fibres

Thermal decomposition parameters were determined from the TG, DTG curves as described below at a heating rate of 5 °C/min. The DTG curves of the untreated and the final nanocellulose powder of jute and PALF are shown in Fig. 4(a) and (b). Here a small weight loss was found in the range of 40–120 °C due to the evaporation of the humidity of the materials or low molecular weight compounds remaining from the isolation procedures. Due to the differences in the chemical structures between hemicellulose, cellulose and lignin, they usually decompose at different temperatures. Many studies related to the decomposition of lignocellulosic materials can be found in specific literature. In the thermal analysis, cellulose decomposition started at 310 °C and persisted until 400 °C (Yang, Yan, Chen, Dong, & Zheng, 2007). In the study of Yang et al., maximum weight loss was reached at 355 °C. At 400 °C almost all cellulose was pyrolyzed, and the solid residuals were relatively small (6.5 wt.%). Hemicellulose started its decomposition at 220 °C and continued up to 300 °C. The decomposition peak reached the maximum mass loss at 268 °C, showing a 20 wt.% of solid residuals at 700 °C. Finally, they showed that lignin decomposition extended to the whole temperature range, starting well below 200 °C and persisting above 700 °C. The solid residue left from lignin pyrolysis was the highest one (46 wt.%). In the present study decomposition of

the untreated fibres of banana, PALF and jute shows several stages, indicating the presence of different components that decompose at different temperatures. The DTG analysis of the banana fibre shows the peaks at 231 °C and 317 °C were caused by hemicellulose and α-cellulose degradation, respectively (Basak et al., 1993). The thermal stability of the natural fibres was decreased when they were subjected to chemical modifications like alkalization (Mitra, Basak, & Sarkar, 1998). But the extracted nanocellulose has an increased thermal stability in the case of banana, jute and PALF fibres. The thermal degradation of nanocellulose obtained from banana fibre shows an increased value, 346 °C, than the raw fibre cellulose of 317 °C. The same trend is observed in the case of PALF and jute fibres. Fig. 4(a) shows the DTG curves of the jute fibre with the degradation of hemicellulose at a temperature of 210 °C and the α-cellulose component of the fibre at 294 °C. Here also the degradation of extracted nanocellulose has a higher value, 326 °C, than the α-cellulose of the untreated raw jute fibre. Fig. 4(b) shows the DTG curves of the PALF with the degradation of hemicellulose at a temperature of 225 °C and the α-cellulose component of the fibre has a value of 313 °C. Here also the degradation of extracted nanocellulose has a higher value, 338 °C, than the α-cellulose of the raw PALF. The wide temperature range observed during lignin decomposition is due to the different activities of the chemical bonds present on its structure (Saito et al., 2006). The lignin–cellulose complex has protected the α-cellulose from degradation to a considerable extent. An increase in residual char formation and lowering of the degradation temperature during the pyrolysis of treated cotton was also reported (Hinojosa, Arthur, & Mares, 1973; Sherly et al., 2008). They explained that this might be caused by an increased rate of formation of free radicals that are stabilized by condensed carbon ring formations in the char (Austen, Ingram, & Tapley, 1958; Hinojosa et al., 1973).

Thus generally nanocelluloses obtained from extracting natural fibres have higher thermal stability than the α-cellulose present in the untreated lignocellulosic fibres. In addition, they showed higher amounts of residual solids. This could be an indicator of the presence of small amounts of hemicellulose or lignin which withstood the extracting procedures.

4. Conclusions

The aim of the work was to suggest a simple and low cost method for the extraction of cellulose from various lignocellulosic fibres and preparation of nanocellulose fibrils from this extracted cellulose. The chemical composition of raw, steam exploded, and bleached fibres was determined. The percentage of cellulose components was found to be increased during steam explosion and the additional bleaching process for all the studied fibres. The lignin and hemicellulose components were found to be decreased from raw to the bleached fibres. Mercerization of the fibre will dissolve the non-crystalline particles from the lignocellulosic fibres. Steam explosion after mercerization of the fibre causes defibrillation and depolymerisation along with isolation of the crystalline cellulose particles. Steam explosion combined with acid hydrolysis has been found to be successful in obtaining fibres in the nano dimension from various plant fibres. A homogenous nanocellulose fibril with a diameter of 5–40 nm is obtained by this process. FTIR, XRD, TGA and morphological analyses clearly support the isolation of nanocellulose fibrils. The crystallinity of the fibre increases during each of these processing steps. Thermal study reveals that thermal stability of the nanocellulose is higher than their respective raw fibres where no lignin cellulose complex is present. By adopting this process it can now be concluded that we can easily isolate the nanocellulose from various lignocellulosic fibres. Out of the three fibres studied; pineapple leaf fibre is the best one for the preparation of nanocellulose fibrils when quality and the yield are concerned. But jute fibre is cheaply and abundantly available and the raw jute fibre has about 60–70% cellulose content. Hence for the cost effective production of nanocellulose, jute fibre is the potential candidate. The prepared nanocellulose fibrils will be a good reinforcement in the polymeric matrices where a large surface area and specific properties of nanotechnology are required (Lima and Borsali, 2004; Zimmermann, Pohler, & Geiger, 2004).

Acknowledgement

The authors are grateful to the Department of Science and Technology (DST), Government of India, for the financial funding of this research work.

Appendix A. Supplementary data

Supplementary data associated with this article can be found, in the online version, at doi:10.1016/j.carbpol.2011.06.034.

References

Austen, D. E. C., Ingram, D. J. E., & Tapley, J. G. (1958). *Faraday Society Transaction*, *54*, 400.
Basak, R. K., Saha, S. G., Sarkar, A. K., Saha, M., Das, N. N., & Mukherjee, A. K. (1993). Thermal properties of jute constituents and flame retardant jute fabrics. *Textiles Research Journal*, *53*, 658–666.
Bhatnagar, A., & Sain, M. (2005). Processing of cellulose nanofiber-reinforced composites. *Journal of Reinforced Plastics and Composites*, *24*, 1259–1268.
Chakraborty, A., Sain, M., & Kortschot, M. (2005). Cellulose nanofibrils: A novel method of preparation using high shear refining and cryocrushing. *Holzforschung*, *59*, 102–107.
Erdtman, H. (2003). Lignins: Occurrence, formation, structure and reactions. *Journal of Polymer Science Part B: Polymer Letters*, *10*, 228–230.
Garcıa, C., Jaldon, G., Dupeyre, D., & Vignon, M. R. (1998). Fibres from semi-retted hemp bundles by steam explosion treatment. *Biomass & Bioenergy*, *14*, 251–260.
Hinojosa, O., Arthur, J. C., & Mares, T. (1973). Thermally initiated free-radical oxidation of cellulose. *Textiles Research Journal*, *43*, 609–614.
Hon, D. N. S. (1994). Cellulose: A random walk along its historical path. *Cellulose*, *1*, 1–25.
Huang, Z. M., Zhang, Y. Z., Kotaki, M., & Ramakrishna, S. (2003). A review on polymer nanofibers by electrospinning and their applications in nanocomposites. *Composites Science and Technology*, *63*, 2223–2253.
Isogai, A., Usuda, M., Kato, T., Uryu, T., & Atalla, H. R. (1989). Solid-state CP/MAS ^{13}C NMR study of cellulose polymorphs. *Macromolecules*, *22*, 3168–3172.
Itoh, T., & Brown, R. M., Jr. (1984). The assembly of cellulose microfibrils in *Valonia macrophysa*. *Planta*, *160*, 372–381.
Kim, N. H., Imai, T., Wada, M., & Sugiyama, J. (2006). Molecular directionality in cellulose polymorphs. *Biomacromolecules*, *7*, 274–280.
Klemm, D., Philipp, B., Heinze, T., Heinze, U., & Wagenknecht, W. (2004). *General considerations on structure and reactivity of cellulose: Section 2.4–2.4.3. Comprehensive cellulose chemistry* Wiley-VCH Verlag GmbH., pp. 130–165
Lima, M. de. S., & Borsali, R. (2004). Rod like cellulose microcrystals: Structure, properties, and applications. *Macromolecular Rapid Communications*, *25*, 771–787.
Lojewska, J., Miskowiec, P., Lojewski, T., & Pronienwicz, L. M. (2005). Cellulose oxidative and hydrolytic degradation: In situ FTIR approach. *Polymer Degradation and Stability*, *88*, 512–520.
Mitra, B. C., Basak, R. K., & Sarkar, M. (1998). Studies on jute-reinforced composites, its limitations, and some solutions through chemical modifications of fibers. *Journal of Applied Polymer Science*, *67*, 1093–1100.
Mohanty, A. K., Misra, M., & Hinrichsen, G. (2000). Biofibres, biodegradable polymers and biocomposites: An overview. *Macromolecular Materials and Engineering*, *276/277*, 1–24.
Mwaikambo, Y., & Ansell, M. P. (1999). The effect of chemical treatment on the properties of hemp, sisal, jute and kapok fibres for composite reinforcement. *Applied Macromolecular Chemistry and Physics*, *272*, 108–116.
Nishino, T., Matsuda, I., & Hirao, K. (2004). All-cellulose composite. *Macromolecules*, *37*, 7683–17683.
Nishiyama, Y., Langan, P., & Chanzy, H. (2002). Crystal structure and hydrogen-bonding system in cellulose Iβ from synchrotron X-ray and neutron fiber diffraction. *Journal of American Chemical Society*, *124*, 9074–9082.
Nishiyama, Y., Sugiyama, J., Chanzy, H., & Langan, P. (2003). Crystal structure and hydrogen bonding system in cellulose I_α from synchrotron X-ray and neutron fiber diffraction. *Journal of the American Chemical Society*, *125*, 14300–14306.
Novak, B. M. (2005). Protein micro patterning via self assembly of nanoparticles. *Advanced Materials*, *17*, 153–155.
Paakko, M., Ankerfors, M., Kosonen, H., Nykanen, A., Ahola, S., Osterberg, M., et al. (2007). Enzymatic hydrolysis combined with mechanical shearing and

high-pressure homogenization for nanoscale cellulose fibrils and strong gels. *Biomacromolecules*, *8*, 1934–1941.
Reddy, N., & Yang, Y. (2005). Structure and properties of high quality natural cellulose fiber from cornstalks. *Polymer*, *46*, 5494–5500.
Saito, T., Nishiyama, Y., Putaux, J. L., Vignon, M., & Isogai, A. (2006). Homogeneous suspensions of individualized microfibrils from TEMPO-catalyzed oxidation of native cellulose. *Biomacromolecules*, *7*, 1687–1691.
Sherly, A. P., Doreen, P., Spange, S., Pothan, L. A., Thomas, S., & Bellmann, C. (2008). Solvatochromic and electrokinetic studies of banana fibrils prepared from steam-exploded banana fiber. *Biomacromolecules*, *9*, 1802–1810.
Subramanian, R., Kononov, A., Kang, T., Paltakari, J., & Paulapuro, H. (2008). Structure and properties of some natural cellulosic fibrils. *Bioresource Technology*, *3*, 192–203.
Taniguchi, T., & Okamura, K. (1998). New films produced from microfibrillated natural fibres. *Polymer International*, *47*, 291–294.
Turbak, A. F., Synder, F. W., & Sandberg, K. R. (1983). Microfibrillated cellulose, a new cellulose product: Properties, uses and commercial potential. In *Journal of Applied Polymer Science. Applied Polymer Symposium, vol. 37* (pp. 815–827).
Xia, Y., Yang, P., Sun, Y., Wu, Y., Mayers, B., Gates, B., et al. (2003). One-dimensional nanostructures: Synthesis, characterization, and applications. *Advanced Materials*, *15*, 353–389.
Yang, H., Yan, R., Chen, H., Dong, Ho. L., & Zheng, C. (2007). Characteristics of hemicellulose, cellulose and lignin pyrolysis. *Fuel*, *86*, 1781–1788.
Zhao, H. P., Feng, X. Q., & Gao, H. (2007). Ultrasonic technique for extracting nanofibers from nature materials. *Applied Physics Letters*, *90*, 073112.
Zimmermann, T., Pohler, E., & Geiger, G. (2004). Cellulose fibrils for polymer reinforcement. *Advanced Engineering Materials*, *6*, 754–761.